S1. Holocene *C. wuellerstorfi* δ^{13}C and sedimentary Pa/Th

At present, NADW extends from 1200 to 4000 m depth in the equatorial Atlantic (Schott, 2003). In Fig. 3, the modern δ^{13}C value of NADW is set to 1.36 ± 0.09 ‰, which is the mean of the δ^{13}C values in benthic foraminifer *C. wuellerstorfi* over the Late Holocene at ~3500 and 2300 m depth on the Brazilian margin. Late Holocene δ^{13}C values are computed as the mean δ^{13}C value over the time interval 0-4 ka (Table S9). This yields Late Holocene δ^{13}C values of 1.30 ± 0.08 ‰ (n = 8) in core MD09-3256Q and 1.43 ± 0.01 ‰ (n = 2) in core MD09-3257.
Modern sedimentary Pa/Th values in Fig. 3 are based on Late Holocene sedimentary Pa/Th measurements in both equatorial cores. The Late Holocene Pa/Th value is of 0.065 ± 0.04 (1 σ) in core MD09-3257 (Burckel et al., 2015) and of 0.043 ± 0.02 (1 σ) in core MD09-3256Q (Table S7). These Pa/Th values are computed using a ^{238}U/^{232}Th lithogenic correction of 0.5 ± 0.1.

S2. Pa/Th uncertainties related to dating uncertainties

The Pa/Th record of core MD09-3257 is used as reference for the definition of the time slices associated with HS2 and Greenland Interstadials. Hence, Pa/Th values associated with the different time slices in core MD09-3257 are independent from the age model. For all other cores, dating uncertainties account for Pa/Th uncertainties associated with each time slice.Studied sediment cores were chosen for their well-defined age model, with uncertainties small enough for their Pa/Th record to be used with confidence. We define the Pa/Th uncertainty associated with each time slice as the maximum between the Pa/Th uncertainty induced by age model uncertainties and induced by averaging Pa/Th values with their own individual uncertainties. At least one Pa/Th value has to be within a specific time slice (considering one sigma uncertainties on the age) for the core Pa/Th data to be used within this time slice.
For core ODP 1063, we considered a 500 y dating uncertainty on the 20-50 ka period (Böhm et al., 2015).
Pa/Th values and uncertainties calculated as detailed in this section are given in Table S3.
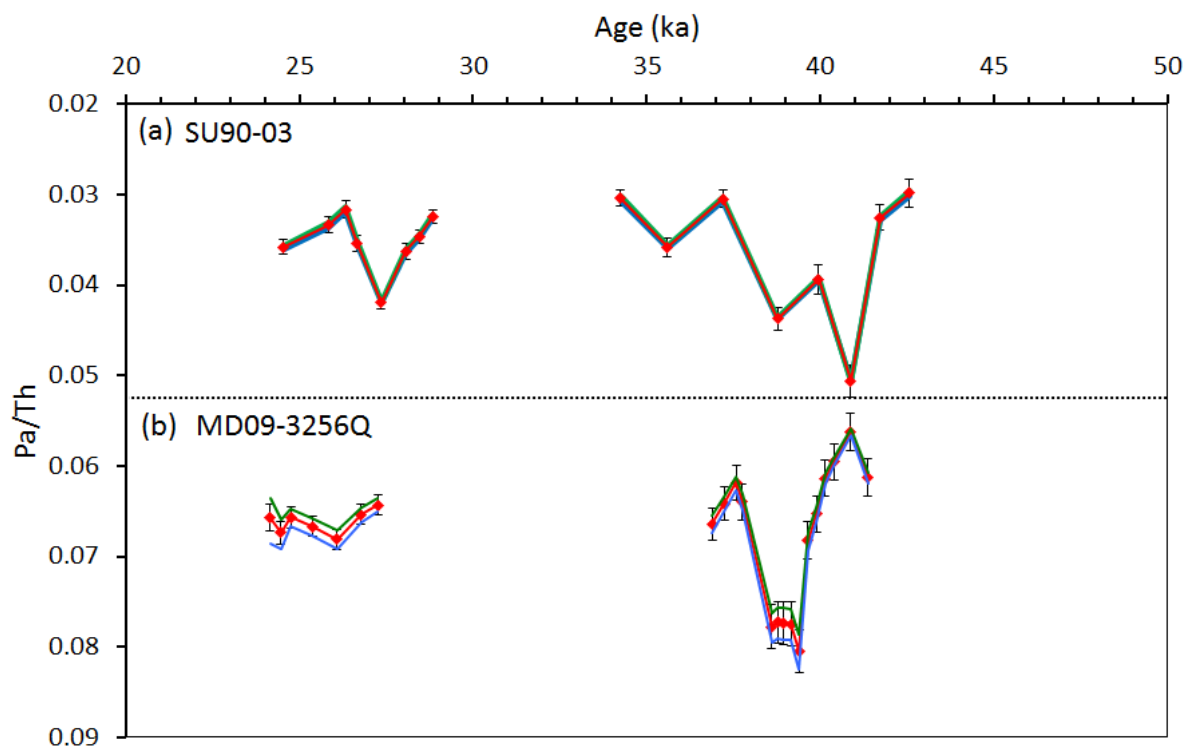
Figure S1: Pa/Th in cores SU90-03 (a) and MD09-3256Q (b) as a function of time calculated with different lithogenic (^{238}U/^{232}Th) (R) values used to correct for detrital material contribution (Francois, 2007). Red curve, R=0.5 (correction used in Fig. 3), green curve R=0.4, and blue curve R=0.6. Error bars are 1 SE and do not account for the error on R.
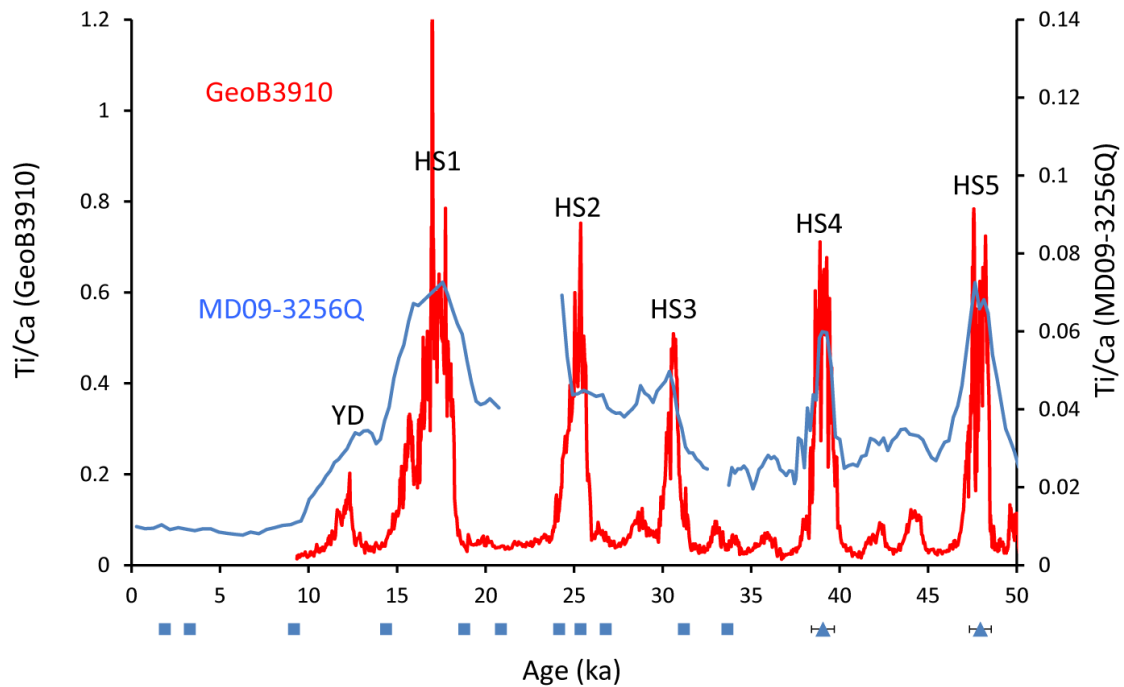
Figure S2: Core MD09-3256Q age model. Blue squares indicate the position of ^{14}C dates in core MD09-3256Q. Blue triangles indicate tie points between core GeoB3910 (red line) and MD09-3256Q (blue line) Ti/Ca records. YD and HS1-HS5 are marked by Ti/Ca peaks caused by increased precipitation and runoff in North-East Brazil during the Younger Dryas and Heinrich Stadials 1-5 (Burckel et al., 2015). Discontinuities in the Ti/Ca record of core MD09-3256Q correspond to the position of turbidite layers. Error bars are 1 sigma and include the uncertainty on correlation for the tie points.
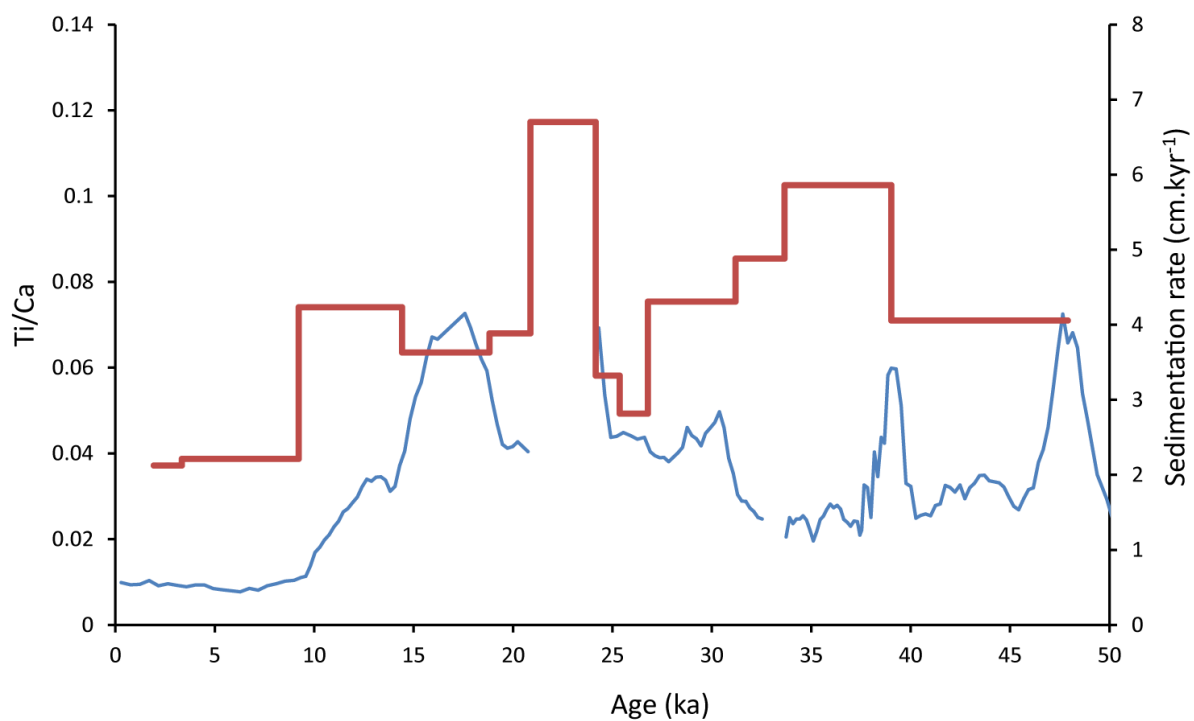
Figure S3: Core MD09-3256Q Ti/Ca record (blue curve) and sedimentation rate (red curve).
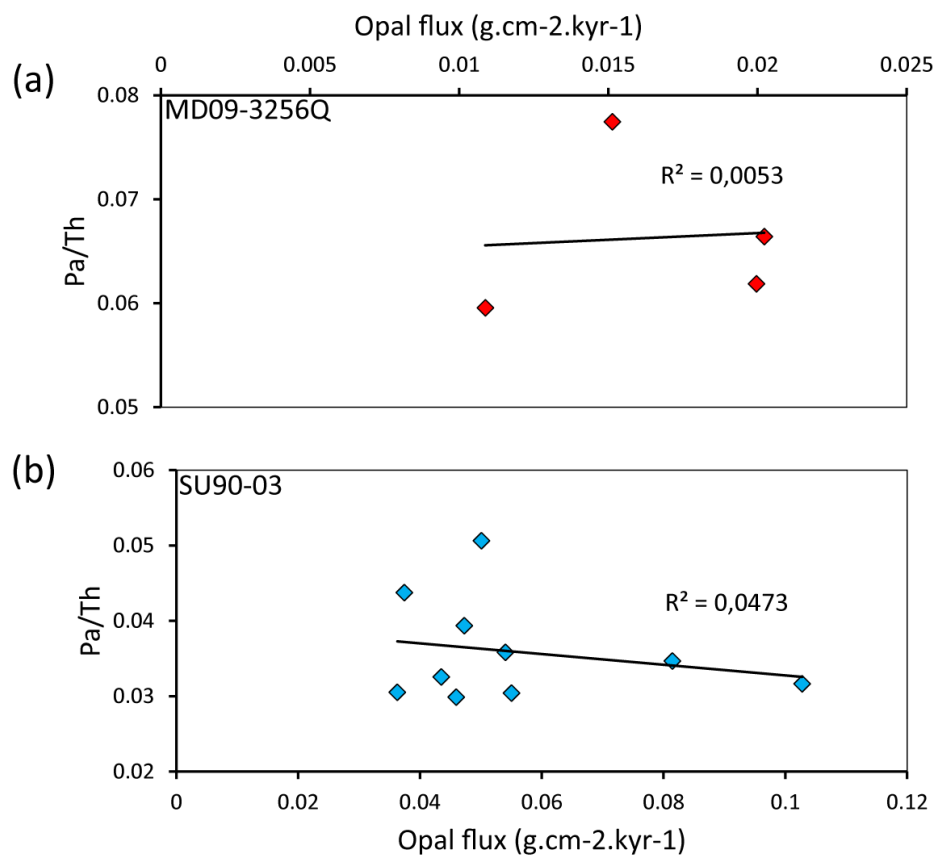
Figure S4: Assessment of the opal influence on the Pa/Th records. Sedimentary Pa/Th as a function of opal flux in core MD09-3256Q (a) and in core SU90-03 (b).
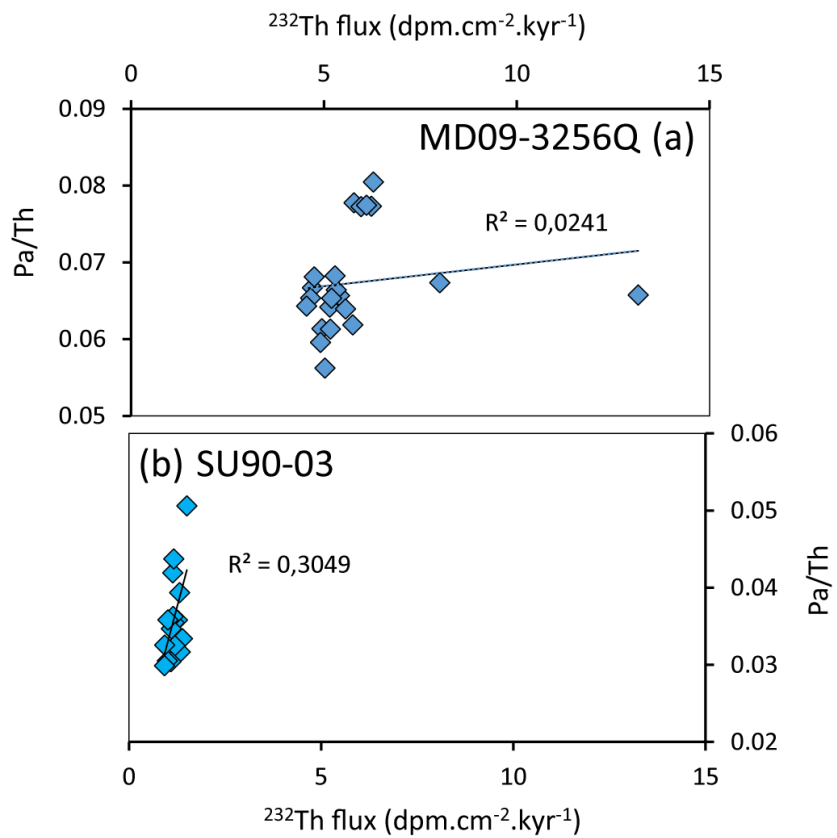
Figure S5: Correlation between the [232]Th flux and sedimentary Pa/Th ratio in (a) core MD09-3256Q, (b) SU90-03.

Shallow overturning simulated Pa/Th
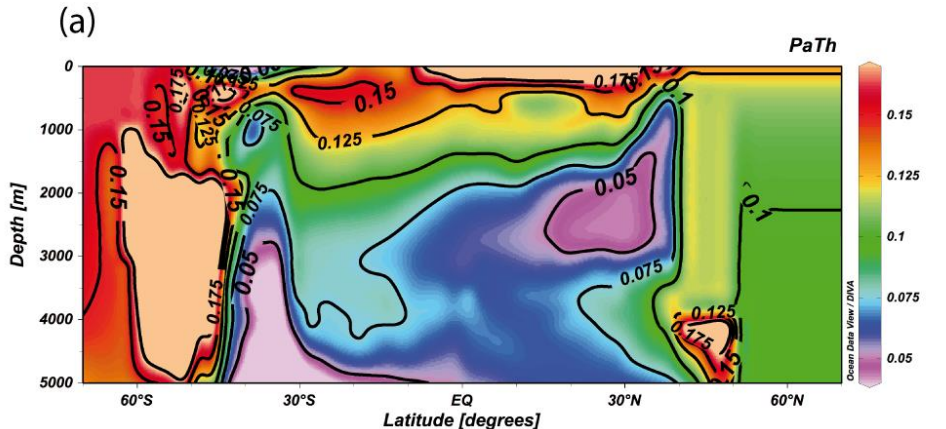
Shallow overturning streamfunction
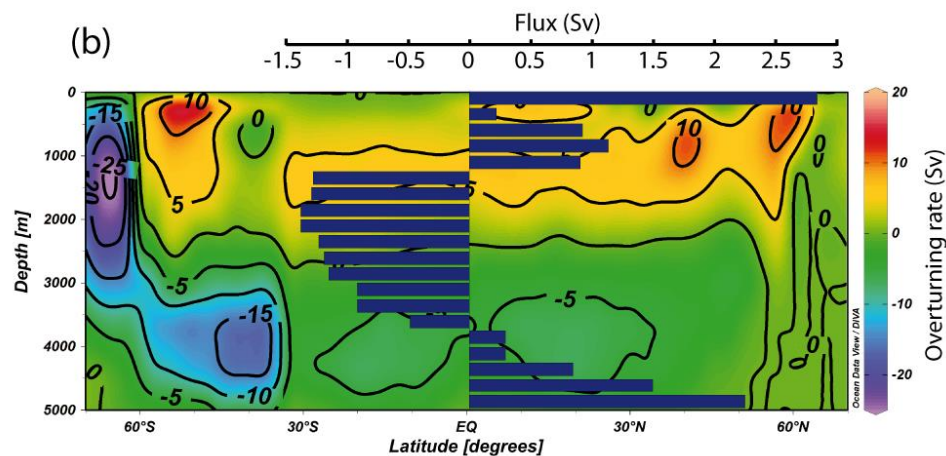
Figure S6: Shallow overturning simulated streamfunction and sedimentary Pa/Th. (a) Simulated sedimentary Pa/Th, (b) simulated streamfunction and flux at the equator (Sv, blue bars, scale on top).
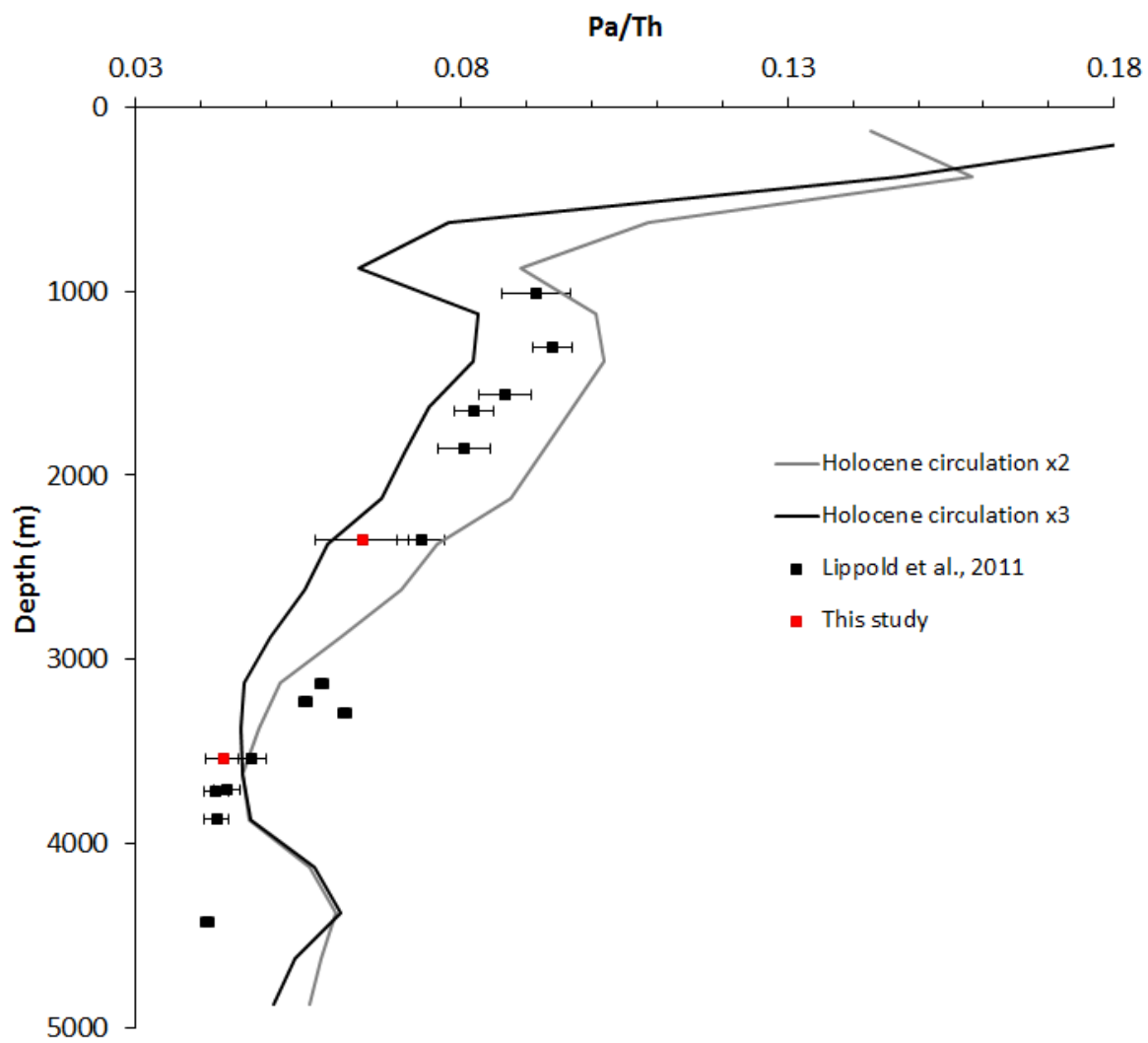
Figure S7: Pa/Th on the Brazilian margin. Red squares are data obtained from Holocene sediments in this study. Black squares are data obtained from Holocene sediments in (Lippold et al., 2011). Grey and black lines are simulated Pa/Th values with the 2 and 3x increased Holocene streamfunction respectively. Error bars are 2 sigma.

8

Table S1: Core locations and age model references.

Core names	Latitude	Longitude	Depth (m)	Age model
MD09-3256Q	03°32.81'S	35°23.11'W	3537	This study
MD09-3257	04°14.69'S	36°21.18'W	2344	(Burckel et al., 2015)
GeoB3910	04°14.7'S	36°20.7'W	2362	(Burckel et al., 2015)
SU90-03	40°30.3'N	32°3.198'W	2475	(Chapman et al., 2000) ^{14}C dates converted to Marine13
ODP 1063	33°41'N	57°37'W	4584	(Böhm et al., 2015)
MD02-2594	34°43'S	17°20'E	2440	(Martínez-Méndez et al., 2010) ^{14}C dates converted to Marine13
V29-172	33°42'N	29°22.98'W	3457	(Bradtmiller et al., 2014)

Table S2: Core MD09-3256Q age model. [14]C ages are measured on planktic foraminifer *G. ruber* (white) and converted to calendar ages using the Marine13 curve (Reimer et al., 2013) with no additional reservoir age correction. * Tie points correlating core MD09-3256Q Ti/Ca to GeoB3910 Ti/Ca.

	Depth (m)	Age 14C (kyr)	1σ	Age (Cal kyr)	1σ
	0.040	2.32	0.03	1.93	0.04
	0.070	3.46	0.03	3.34	0.04
	0.200	8.575	0.035	9.22	0.07
	0.420	12.79	0.05	14.41	0.18
	0.580	15.97	0.06	18.82	0.06
	0.660	17.72	0.06	20.88	0.11
	0.880	20.5	0.08	24.16	0.12
	0.920	21.41	0.08	25.36	0.12
	0.960	22.87	0.08	26.79	0.18
	1.150	27.69	0.21	31.19	0.13
	1.270	29.85	0.27	33.65	0.25
*	1.585	/		39.03	0.65
*	1.945	/		47.91	0.62

Table S3: Pa/Th for each time slice in the different cores. Uncertainties are calculated as specified in Sect. S2.

	HS2	1 σ	GI-3	1 σ	GI -8	1 σ	GI-10	1 σ
MD09-3256Q	0.067	0.005	0.064	0.004	0.064	0.006	0.059	0.005
MD09-3257	0.102	0.011	0.072	0.009	0.066	0.010	0.075	0.009
SU90-03	0.033	0.002	0.038	0.04	0.037	0.009	0.040	0.015
ODP1063	0.079	0.007	0.068	0.006	0.071	0.016	na	na
MD02-2594	na	na	0.046	0.005	0.049	0.005	0.049	0.004
V29-172	na	na	0.040	0.002	na	na	na	na

Table S4: Euclidean distance between simulated and measured Pa/Th values in all Atlantic cores for the different times slices. Streamfunctions are multiplied by factors of 1, 2 and 3, where 1 means no change in the streamfunction simulated by the iLOVECLIM model. For each time slice, the best fit between modeled and measured Pa/Th data is displayed in bold.

	HS2	1 σ	GI-3	1 σ	GI -8	1 σ	GI-10	1 σ
Shallow x1	0.089	0.005	0.091	0.004	0.081	0.009	0.078	0.014
Shallow x2	0.100	0.006	0.100	0.004	0.080	0.009	0.079	0.014
Shallow x3	0.107	0.007	0.102	0.004	0.085	0.010	0.083	0.014
off mode x1	0.121	0.003	0.162	0.004	0.132	0.010	0.123	0.013
off mode x2	0.133	0.003	0.163	0.005	0.145	0.009	0.138	0.013
off mode x3	0.111	0.003	0.132	0.005	0.123	0.009	0.117	0.013
Holocene x1	**0.039**	0.004	0.060	0.006	0.061	0.008	0.054	0.009
Holocene x2	**0.047**	0.007	**0.044**	0.004	**0.041**	0.008	**0.035**	0.011
Holocene x3	0.059	0.009	**0.049**	0.004	**0.038**	0.010	**0.033**	0.012

Table S5: Euclidean distances between simulated and measured Pa/Th values in all Atlantic cores, not considering the intermediate and deep mid-latitude North Atlantic cores SU90-03 and V29-172, for the different times slices.

	HS2	1 σ	GI-3	1 σ	GI -8	1 σ	GI-10	1 σ
Shallow x1	**0.034**	0.011	**0.025**	0.005	**0.021**	0.008	**0.023**	0.005
Shallow x2	0.057	0.011	**0.025**	0.008	**0.020**	0.010	**0.027**	0.009
Shallow x3	0.067	0.010	**0.037**	0.008	**0.034**	0.010	0.037	0.008
off mode x1	0.046	0.007	0.076	0.007	0.077	0.010	0.065	0.007
off mode x2	**0.033**	0.010	0.070	0.008	0.074	0.009	0.066	0.008
off mode x3	**0.028**	0.010	0.064	0.008	0.068	0.009	0.060	0.008
Holocene x1	**0.019**	0.007	0.052	0.006	0.054	0.008	0.047	0.006
Holocene x2	**0.034**	0.009	**0.032**	0.005	**0.030**	0.007	**0.025**	0.004
Holocene x3	0.048	0.010	**0.030**	0.006	**0.025**	0.011	**0.021**	0.007

Table S6: Opal data in cores SU90-03 and MD09-3256Q.

Core	Depth (cm)	Age (ka)	Opal (wt%)	Opal flux (g.cm^{-2}.kyrs^{-1})
SU90-03	133	26.328	6.7	0.103
SU90-03	145	28.454	5.8	0.081
SU90-03	180	34.247	3.9	0.055
SU90-03	185	35.599	3.7	0.054
SU90-03	190	37.190	2.6	0.036
SU90-03	195	38.780	2.5	0.037
SU90-03	200	39.942	3.0	0.047
SU90-03	205	40.868	3.2	0.050
SU90-03	210	41.713	3.1	0.044
SU90-03	215	42.558	3.3	0.046
MD09-3256Q	146	36.893	0.7	0.020
MD09-3256Q	150	37.576	0.7	0.020
MD09-3256Q	159	39.149	0.7	0.015
MD09-3256Q	159	39.149	0.7	0.015
MD09-3256Q	164	40.382	0.4	0.011

Table S7: Pa/Th and isotopic concentrations (dpm.g^{-1}) in core MD09-3256Q. Pa/Th values are computed using a $^{238}U/^{232}Th$ lithogenic correction of 0.5 ± 0.1. 0.5 ky uncertainty was attributed to the core top extrapolated age.

Depth (m)	Age (Cal kyr BP)	1 σ	231Pa	1 SE	230Th	1 SE	232Th	1 SE	238U	1 SE	Pa/Th	1 SE
0	0.05	0.50	0.240	0.001	5.49	0.04	1.190	0.008	1.079	0.006	0.043	0.002
0	0.05	0.50	0.240	0.002	5.51	0.03	1.198	0.007	1.075	0.005	0.043	0.002
0.88	24.16	0.12	0.181	0.002	3.76	0.02	3.460	0.017	1.904	0.006	0.066	0.012
0.89	24.46	0.12	0.241	0.003	4.91	0.02	3.393	0.015	1.802	0.006	0.067	0.008
0.9	24.76	0.12	0.246	0.003	5.08	0.03	2.760	0.014	1.344	0.004	0.066	0.005
0.9	24.76	0.12	0.245	0.003	5.13	0.03	2.641	0.013	1.332	0.004	0.065	0.005
0.92	25.36	0.12	0.259	0.003	5.35	0.03	2.565	0.014	1.253	0.004	0.067	0.005
0.94	26.08	0.15	0.267	0.003	5.44	0.03	2.632	0.015	1.380	0.004	0.068	0.005
0.96	26.79	0.18	0.254	0.003	5.37	0.03	2.558	0.014	1.430	0.004	0.065	0.005
0.98	27.25	0.17	0.241	0.003	5.19	0.03	2.447	0.010	1.312	0.005	0.064	0.004
1.46	36.89	0.49	0.151	0.002	3.41	0.02	1.904	0.012	1.130	0.008	0.066	0.006
1.48	37.23	0.51	0.152	0.002	3.55	0.03	1.947	0.013	1.122	0.007	0.064	0.005
1.5	37.58	0.54	0.150	0.002	3.59	0.03	2.145	0.013	1.394	0.007	0.061	0.006
1.5	37.58	0.54	0.152	0.002	3.53	0.02	2.004	0.012	1.367	0.008	0.063	0.006
1.51	37.75	0.55	0.160	0.002	3.63	0.03	2.024	0.013	1.602	0.011	0.064	0.006
1.56	38.60	0.61	0.226	0.003	4.55	0.03	2.595	0.016	2.117	0.011	0.078	0.007
1.57	38.77	0.63	0.233	0.003	4.81	0.02	2.913	0.012	1.820	0.006	0.077	0.007
1.58	38.94	0.64	0.232	0.003	4.81	0.03	3.040	0.016	1.746	0.006	0.078	0.007
1.59	39.15	0.64	0.235	0.003	4.66	0.04	2.948	0.021	1.645	0.009	0.083	0.007
1.59	39.15	0.64	0.213	0.003	4.67	0.03	2.888	0.017	1.637	0.008	0.072	0.007
1.6	39.40	0.64	0.230	0.003	4.70	0.03	3.050	0.012	1.491	0.005	0.081	0.007
1.61	39.64	0.64	0.186	0.002	4.26	0.03	2.444	0.012	1.265	0.004	0.068	0.006
1.62	39.89	0.64	0.176	0.002	4.13	0.02	2.327	0.010	1.289	0.004	0.065	0.006
1.63	40.14	0.64	0.155	0.002	3.80	0.02	2.042	0.012	1.272	0.007	0.061	0.005
1.64	40.38	0.64	0.150	0.002	3.74	0.02	2.003	0.011	1.247	0.008	0.059	0.005
1.66	40.87	0.64	0.146	0.002	3.76	0.03	2.038	0.014	1.352	0.007	0.056	0.005
1.68	41.37	0.64	0.148	0.002	3.66	0.02	2.057	0.012	1.210	0.006	0.061	0.006

Table S8: Pa/Th and isotopic concentrations (dpm.g^{-1}) in core SU90-03. Pa/Th values are computed using a $^{238}U/^{232}Th$ lithogenic correction of 0.5 ± 0.1. 1 ky uncertainty was attributed to extrapolated ages (lower part of the core below 2.09 m, Chapman et al., 2000).

Depth (m)	Age (Cal kyr BP)	1 σ	231Pa	1 SE	230Th	1 SE	232Th	1 SE	238U	1 SE	Pa/Th	1 SE
1.27	24.534	0.148	0.138	0.001	4.07	0.06	0.784	0.004	2.113	0.005	0.036	0.002
1.31	25.832	0.155	0.132	0.002	4.10	0.04	0.870	0.007	2.083	0.016	0.033	0.002
1.33	26.328	0.153	0.130	0.002	4.23	0.07	0.873	0.009	2.038	0.014	0.032	0.002
1.35	26.670	0.147	0.147	0.002	4.59	0.05	0.902	0.010	2.066	0.015	0.035	0.002
1.35	26.670	0.147	0.151	0.001	4.55	0.07	0.789	0.004	2.143	0.005	0.036	0.001
1.39	27.354	0.133	0.168	0.001	4.54	0.05	0.809	0.004	2.352	0.005	0.042	0.002
1.43	28.075	0.129	0.148	0.002	4.43	0.05	0.799	0.004	2.233	0.005	0.036	0.002
1.45	28.454	0.131	0.144	0.001	4.47	0.05	0.781	0.004	2.178	0.005	0.035	0.001
1.47	28.833	0.133	0.129	0.001	4.19	0.06	0.796	0.004	1.980	0.004	0.032	0.001
1.8	34.247	0.341	0.125	0.001	4.32	0.04	0.776	0.004	1.977	0.004	0.030	0.002
1.85	35.599	0.394	0.123	0.002	4.04	0.04	0.699	0.004	1.583	0.003	0.036	0.002
1.9	37.190	0.445	0.107	0.001	4.06	0.04	0.715	0.004	1.354	0.003	0.031	0.001
1.95	38.780	0.497	0.126	0.002	3.82	0.04	0.786	0.004	1.250	0.003	0.044	0.002
2	39.942	0.534	0.102	0.002	3.46	0.05	0.829	0.004	0.888	0.002	0.039	0.002
2.05	40.868	0.523	0.119	0.002	3.46	0.05	0.954	0.005	0.766	0.002	0.051	0.003
2.1	41.713	1.000	0.092	0.001	3.72	0.05	0.660	0.003	0.845	0.002	0.033	0.002
2.15	42.558	1.000	0.098	0.002	3.87	0.05	0.660	0.003	1.272	0.003	0.030	0.002

Table S9: Core MD09-3256Q δ¹³C (*C. wuellerstorfi*)

Age (Cal kyr BP)	Depth (m)	∂¹³C (‰)	Age (Cal kyr BP)	Depth (m)	∂¹³C (‰)	Age (Cal kyr BP)	Depth (m)	∂¹³C (‰)
0.52	0.01	1.13	27.48	0.99	0.20	36.21	1.42	0.51
1.46	0.03	1.38	27.71	1	0.07	36.38	1.43	0.67
1.93	0.04	1.29	27.95	1.01	0.29	36.55	1.44	0.65
1.93	0.04	1.33	27.95	1.01	0.08	36.72	1.45	0.86
2.40	0.05	1.28	28.18	1.02	0.25	36.89	1.46	0.96
2.87	0.06	1.28	28.41	1.03	0.33	37.06	1.47	0.40
3.34	0.07	1.36	28.64	1.04	0.15	37.23	1.48	0.55
3.80	0.08	1.34	28.87	1.05	0.38	37.40	1.49	0.42
20.11	0.63	0.23	29.11	1.06	0.40	37.40	1.49	0.59
20.36	0.64	0.30	29.34	1.07	0.45	37.58	1.5	0.68
20.36	0.64	0.21	29.34	1.07	0.08	37.75	1.51	0.53
20.62	0.65	0.31	29.57	1.08	0.34	37.92	1.52	0.44
20.88	0.66	0.23	29.57	1.08	0.37	38.09	1.53	0.19
21.03	0.67	0.09	30.03	1.1	0.48	38.26	1.54	0.40
21.18	0.68	0.12	30.27	1.11	0.50	38.43	1.55	0.71
21.33	0.69	0.31	30.50	1.12	0.45	38.60	1.56	0.26
21.33	0.69	0.33	30.73	1.13	0.33	38.77	1.57	0.43
21.48	0.7	0.29	30.96	1.14	0.35	38.94	1.58	0.22
21.77	0.72	0.03	31.19	1.15	0.36	39.15	1.59	0.22
21.77	0.72	0.36	31.40	1.16	0.68	39.40	1.6	0.40
21.92	0.73	0.25	31.60	1.17	0.58	39.64	1.61	0.31
22.07	0.74	0.32	31.60	1.17	0.42	39.89	1.62	0.29
22.22	0.75	0.16	31.81	1.18	0.25	39.89	1.62	0.21
22.37	0.76	0.17	32.01	1.19	0.71	40.14	1.63	0.30
22.37	0.76	0.25	32.22	1.2	0.62	40.38	1.64	0.38
22.52	0.77	0.29	32.42	1.21	0.25	40.63	1.65	0.52
22.67	0.78	0.31	32.63	1.22	0.33	40.63	1.65	0.27
22.82	0.79	0.30	32.83	1.23	0.56	40.87	1.66	0.13
22.82	0.79	0.18	33.04	1.24	0.68	41.12	1.67	0.57
22.97	0.8	0.24	33.24	1.25	0.56	41.12	1.67	0.33
23.12	0.81	0.21	33.45	1.26	0.70	41.37	1.68	0.80
23.27	0.82	0.08	33.45	1.26	0.50	41.37	1.68	0.71
23.27	0.82	0.09	33.65	1.27	0.83	41.61	1.69	0.41
23.41	0.83	0.16	33.82	1.28	0.41	41.61	1.69	0.55
23.56	0.84	0.12	33.82	1.28	0.53	41.86	1.7	0.88
23.71	0.85	0.02	33.82	1.28	0.58	41.86	1.7	0.77
23.86	0.86	-0.03	33.99	1.29	0.56	42.35	1.72	0.28
24.01	0.87	0.25	34.16	1.3	0.48	42.35	1.72	1.20
24.16	0.88	0.30	34.33	1.31	0.53	42.85	1.74	0.98
24.16	0.88	0.14	34.50	1.32	0.17	43.34	1.76	0.80
24.16	0.88	0.08	34.68	1.33	0.40	43.83	1.78	0.73
24.46	0.89	-0.16	34.85	1.34	0.77	43.83	1.78	0.56
25.06	0.91	0.34	35.02	1.35	0.68	44.33	1.8	0.33
25.36	0.92	0.10	35.19	1.36	0.40	44.33	1.8	0.70
25.72	0.93	0.12	35.36	1.37	0.56			
26.08	0.94	0.39	35.36	1.37	0.49			
26.43	0.95	0.31	35.53	1.38	0.42			
26.79	0.96	0.23	35.70	1.39	0.56			
27.02	0.97	0.39	35.87	1.4	0.43			
27.25	0.98	0.44	36.04	1.41	0.55			

Additional references

Böhm, E., Lippold, J., Gutjahr, M., Frank, M., Blaser, P., Antz, B., Fohlmeister, J., Frank, N., Andersen, M. B. and Deininger, M.: Strong and deep Atlantic meridional overturning circulation during the last glacial cycle, Nature, 517(7532), 73–76 [online] Available from: http://dx.doi.org/10.1038/nature14059, 2015.

Bradtmiller, L. I., McManus, J. F. and Robinson, L. F.: 231Pa/230Th evidence for a weakened but persistent Atlantic meridional overturning circulation during Heinrich Stadial 1, Nat. Commun., 5, 5817, doi:10.1038/ncomms6817, 2014.

Burckel, P., Waelbroeck, C., Gherardi, J. M., Pichat, S., Arz, H., Lippold, J., Dokken, T. and Thil, F.: Atlantic Ocean circulation changes preceded millennial tropical South America rainfall events during the last glacial, Geophys. Res. Lett., 42(2), 411–418, doi:10.1002/2014GL062512, 2015.

Chapman, M. R., Shackleton, N. J. and Duplessy, J.-C.: Sea surface temperature variability during the last glacial–interglacial cycle: assessing the magnitude and pattern of climate change in the North Atlantic, Palaeogeogr. Palaeoclimatol. Palaeoecol., 157(1–2), 1–25, doi:http://dx.doi.org/10.1016/S0031-0182(99)00168-6, 2000.

Francois, R.: Paleoflux and Paleocirculation from Sediment 230Th and 231Pa/230Th, in Proxies in Late Cenozoic Paleoceanography, vol. 1, pp. 681–716, Elsevier., 2007.

Lippold, J., Gherardi, J. M. and Luo, Y.: Testing the 231Pa/230Th paleocirculation proxy: A data versus 2D model comparison, Geophys. Res. Lett., 38(20), 1–7, doi:10.1029/2011GL049282, 2011.

Martínez-Méndez, G., Zahn, R., Hall, I. R., Peeters, F. J. C., Pena, L. D., Cacho, I. and Negre, C.: Contrasting multiproxy reconstructions of surface ocean hydrography in the Agulhas Corridor and implications for the Agulhas Leakage during the last 345,000 years, Paleoceanography, 25(4), 1-12, doi:10.1029/2009PA001879, 2010.

Reimer, P. J., Bard, E., Bayliss, A., Beck, J. W., Blackwell, P. G., Ramsey, C. B., Buck, C. E., Cheng, H., Edwards, R. L., Friedrich, M., Grootes, P. M., Guilderson, T. P., Haflidason, H., Hajdas, I., Hatte, C., Heaton, T. J., Hoffmann, D. L., Hogg, A. G., Hughen, K. A., Kaiser, K. F., Kromer, B., Manning, S. W., Niu, M., Reimer, R. W., Richards, D. A., Scott, E. M., Southon, J. R., Staff, R. A., Turney, C. S. M. and van der Plicht, J.: IntCal13 and Marine13 Radiocarbon Age Calibration Curves 0–50,000 years Cal BP, Radiocarbon, 55(4), 1869–1887 [online] Available from: http://apps.webofknowledge.com.biblioplanets.gate.inist.fr/full_record.do?product=UA&search_mode=GeneralSearch&qid=12&SID=R2qElS8CFcTUu7uanDW&page=1&doc=2 (Accessed 1 July 2015), 2013.

Schott, F. a.: The zonal currents and transports at 35°W in the tropical Atlantic, Geophys. Res. Lett., 30(7), 35–38, doi:10.1029/2002GL016849, 2003.